Chemical Engineering Journal 146 (2009) 189–193

Contents lists available at ScienceDirect

Chemical Engineering Journal

journal homepage: www.elsevier.com/locate/cej

Numerical finite volume modeling of dye decolorization using immobilized titania nanophotocatalysis

Niyaz Mohammad Mahmoodi [a,*], Mokhtar Arami [b]

[a] Department of Organic Colorants, Institute for Colorants, Paint and Coatings, Tehran, Iran
[b] Textile Engineering Department, Amirkabir University of Technology, Tehran, Iran

ARTICLE INFO

Article history:
Received 4 March 2007
Received in revised form 17 May 2008
Accepted 23 May 2008

Keywords:
Numerical finite volume
Nanophotocatalysis
Modeling
Decolorization
Textile dyes
Immobilized titania nanoparticle

ABSTRACT

This paper presents a numerical finite volume model for simulation of decolorization and mineralization of dyes by nanophotocatalysis using immobilized titania. Three textile dyes, Remazol Red RB (RR), Remazol Brilliant Blue BB (RBB) and Cibacron Blue TGRE (CB), were used as model compounds. UV–vis, ion chromatography (IC) and chemical oxygen demand (COD) analyses were employed to obtain the details of the photocatalytic degradation of dyes. Numerical finite volume model was used to solve the mathematical equation describing decolorization process. The results showed that the dyes were decolorized and mineralized. The model predictions were compared to those results obtained from experimental tests and close agreement was achieved.

1. Introduction

The presence of harmful compounds in water supplies and wastewater from chemical industries such as textile, power plants, and agricultural sources is a global concern. Waste effluents emanating from textile industry create serious problems to various segments of the environment. Dyes in waters affect the nature of the water, inhibiting light penetration into the streams and reducing the photosynthetic reaction. Some dyes are toxic and even at very low concentrations may significantly affect aquatic life. Some other dyes may cause allergy, skin irritation and cancer to humans [1–7].

Processes based on aqueous phase hydroxyl radical chemistry are powerful oxidation methods to destroy toxic organic compounds present in water [8–29]. Nanophotocatalysis using titania is one of the advanced oxidation processes that couples low-energy ultraviolet light with semiconductors acting as photocatalysts. During the photocatalytic reactions, valence band hole (h_{vb}^+) and hydroxyl radical ($OH^\bullet$) are produced [30,31]. The h_{vb}^+ is a strong oxidant, which can either oxidize a compound directly or react with electron donors like water or hydroxide ions to form hydroxyl radicals, which react with pollutants such as dyes. Hydroxyl radicals react with organic pollutants leading to the total mineralization of most of them.

In numerous investigations, an aqueous suspension of the catalyst particles in immersion or annular-type photoreactors has been used. However, the use of suspensions requires the separation and recycling of the ultrafine catalyst from the treated liquid. These processes are usually inconvenient, time-consuming and expensive. In addition, the depth of penetration of UV light is limited because of strong absorption by catalyst and dissolved pollutants. One solution to the above problem is to immobilize the catalyst onto a fixed transparent support [32].

Literature review showed that numerical finite volume modeling of photocatalytic decolorization of dyes using immobilized titania was not done. The main objective of this paper is to investigate the numerical finite volume model for photocatalytic decolorization of dyes using immobilized titania. A multi-purpose CFD package called PHOENICS [33] incorporating the numerical finite volume approach was used to simulate the photocatalytic decolorization process. Ion chromatography (IC) and chemical oxygen demand (COD) analyses were employed to obtain the details of the photocatalytic degradation of dyes.

2. Experimental

Remazol Red RB (RR), Remazol Brilliant Blue BB (RBB) and Cibacron Blue TGRE (CB) were obtained from Hoechst and Ciba. Other chemicals were of analar grade and purchased from Merck.

* Corresponding author. Tel.: +98 21 22956126; fax: +98 21 22947537.
E-mail address: nm_mahmoodi@yahoo.com (N.M. Mahmoodi).

1385-8947/$ – see front matter © 2008 Elsevier B.V. All rights reserved.
doi:10.1016/j.cej.2008.05.036

Nanosized titania (Degussa P25) was utilized as photocatalyst. Its main physical data are as follows: average primary particle size 30 nm, purity above 97% and with 80:20 anatase to rutile.

Experiments were carried out in an immersion rectangular immobilized TiO_2 nanoparticle photocatalytic reactor made of Pyrex glass [1,3,5]. Two UV-C lamps (15 W, Philips) were used as the radiation source. An air pump was utilized for the mixing and aeration of dye solution.

Photocatalytic decolorization and mineralization processes were performed using a 6 L solution containing specified concentration of dye. Solutions were prepared using distilled water to minimize interferences. The initial dye concentration was 50 mg/L. The photocatalytic degradation was carried out at 298 K. Samples were withdrawn from sample point at certain time intervals and analysed for decolorization and mineralization.

Decolorization of dye solutions were checked and controlled by measuring the absorbance of dyes at their maximum wavelengths at different time intervals by UV–vis CECIL 2021 spectrophotometer. The maximum wavelength (λ_{max}) of RR, RBB and CB were 520, 608 and 580 nm, respectively.

Computational fluid dynamics based on finite volume descretization scheme was used to numerically solve the mathematical equation describing decolorization process.

Ion chromatograph (METROHM 761 Compact IC) was used to assay the appearance and quantity of formate, acetate, oxalate, SO_4^{2-} and NO_3^- ions formed during the decolorization and mineralization of dyes using a METROSEP anion dual 2, flow 0.8 ml/min, 2 mM $NaHCO_3$/1.3 mM Na_2CO_3 as eluent, temperature 20 °C, pressure 3.4 MPa and conductivity detector.

The COD tests were carried out according to close reflux, colorimetric method [34] using a DR/2500 spectrophotometer (Hach, USA) and COD reactor (Hach, USA).

3. Results and discussions

3.1. Decolorization process

Figs. 1–3 (dots) show the dye concentration as a function of the irradiation time for RR, RBB and CB, respectively. Different H_2O_2 concentrations were used. It is shown to be exponential to time at each concentration of H_2O_2. This means that the first order kinetics relative to dye is operative. The correlation coefficient (R^2) and decolorization rate constants (k, min^{-1}) of dye for the various H_2O_2 concentrations were shown in Table 1. Apparently, as H_2O_2 concentration increases from 0 to optimal concentration (450, 450 and 300 mg/L for RR, RBB and CB, respectively), the decolorization rate is greatly enhanced because more hydroxyl radicals are formed at higher hydrogen peroxide concentrations in solution.

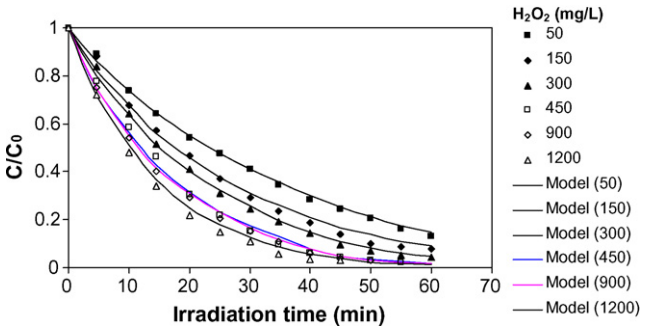

Fig. 2. Comparison of concentrations of RBB versus irradiation time in aqueous phase for different concentrations of hydrogen peroxide and an initial dye concentration (C_0) 50 mg/L predicted by numerical model (solid lines) and determined at laboratory (dots).

However, when H_2O_2 concentration is larger than optimal concentration, the decolorization rate slows down. This can be explained by the scavenging effect when using a higher H_2O_2 concentration on the further generation of hydroxyl radicals in aqueous solution [1,3,10].

3.2. Computational fluid dynamics modeling of decolorization process

In this paper a computational fluid dynamics based on finite volume descretization scheme was used to numerically solve the mathematical equation describing decolorization process. The partial differential equation describing the photocatalytic decolorization process is given in the following equation. This equation was numerically solved using PHOENICS package and incorporating finite volume integration scheme in order to simulate the decolorization from aqueous solution.

$$\frac{\partial C_1}{\partial t} = D\frac{\partial^2 C_1}{\partial x^2} - kC_1 \quad (1)$$

where C_1 is the dye concentration in aqueous system (mg/L), k the first-order rate constant (1/s), t the time (s), x the Cartesian coordinates (m) and D is the diffusion coefficient (m^2/s).

To produce a CFD modeling, a number of key steps should be followed in order to generate an exact picture of a particular problem. The main steps for a CFD analysis are [33]:

- *Start*
- *Identification of the problems to be analysed and derivation of a conceptual model*

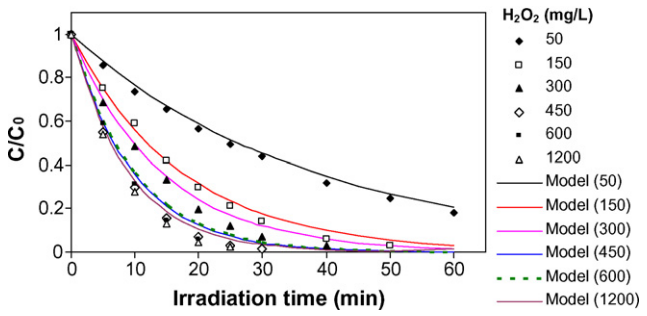

Fig. 1. Comparison of concentrations of RR versus irradiation time in aqueous phase for different concentrations of hydrogen peroxide and an initial dye concentration (C_0) 50 mg/L predicted by numerical model (solid lines) and determined at laboratory (dots).

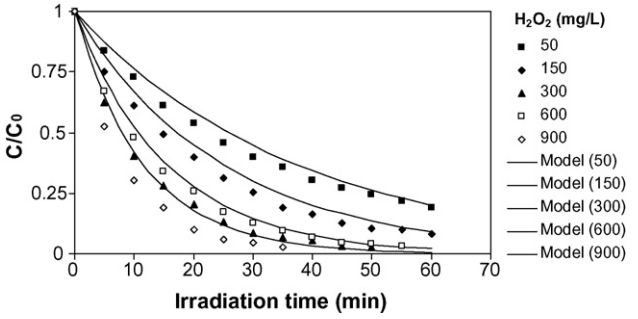

Fig. 3. Comparison of concentrations of CB versus irradiation time in aqueous phase for different concentrations of hydrogen peroxide and an initial dye concentration (C_0) 50 mg/L predicted by numerical model (solid lines) and determined at laboratory (dots).

Table 1
First-order kinetics rate constants for photocatalytic decolorization of dyes

H_2O_2 (mg/L)	RR		RBB		CB	
	k (1/min)	R^2	k (1/min)	R^2	k (1/min)	R^2
50	0.028	0.999	0.032	0.994	0.029	0.991
150	0.067	0.990	0.043	0.993	0.044	0.992
300	0.085	0.993	0.051	0.991	**0.076**	0.990
450	**0.135**	0.990	**0.067**	0.990	–	–
600	0.132	0.996	–	–	0.066	0.992
900	–	–	0.068	0.990	0.107	0.991
1200	0.139	0.991	0.069	0.993	–	–

- *Pre-processing phase* (*1. Construction of the problem domain and grid generation*; *2. Specification of boundary conditions and fluid properties*)
- *Solution phase* (*Numerical solution of the problem*)
- *Pre-processing phase* (*Result evaluation*).

The equation describing photocatalytic decolorization of dyes in solution phase was solved using the PHOENICS CFD package. PHOENICS is a general-purpose CFD package that can be used for the simulation of fluid flow, heat transfer and mass transfer processes. In the case of a single-phase problem, the partial differential equation solved by PHOENICS has the following general form [33]:

$$\frac{\partial}{\partial t}(\rho\phi) + \frac{\partial}{\partial x_j}\left(\rho U_j\phi - \Gamma_\phi \frac{\partial \phi}{\partial x_j}\right) = S_\phi \quad (2)$$

where ϕ is any of the dependent variable, t the time, ρ the PHOENICS term for density, U_j the velocity component in the x_j direction, Γ_ϕ the diffusive exchange coefficient for ϕ and S_ϕ is the source rate of ϕ.

The general source term S_ϕ can include all terms other than diffusion, convection and transient terms in the equation.

Boundary conditions and sources or sinks (S_{bc}) are treated in PHOENICS as linearized sources having the following form [33]:

$$S_{bc} = TC'(V - \phi) \quad (3)$$

where C' is the coefficient, V the value and T is the type, a geometrical multiplier.

The PHOENICS computer model has a few different modules for performing all of the different phases of a numerical analysis, namely SATELLITE (definition of geometry, grid generation, selection of the physical and chemical phenomena that need to modelled, definition of fluid properties and specification of boundary conditions), EARTH (descretization of finite volume equations, iterative solution of finite volume equations, output of results) and post-processing facilities including VR VIEWER (viewing streamlines, vectors, iso-surfaces and contour plots), PHOTON (viewing grid streamlines, vector plots, surface plots and contour plots), AUTOPLOT (plot x–y graphs for comparison of PHOENICS solutions with field data) and RESULT (drawing tabular plots of unknown variables) [33].

Table 2
Model input data used for the simulation of photocatalytic decolorization of dyes

Input parameter	Value
Initial dye concentration (mg/L)	50
Kinetic rate constant (1/min)	Table 1
Molecular diffusion (m^2/s)	1×10^{-9}
Number of iterations	1000
Number of time steps	12
PHOENICS-term for density (g/cm^3)	1.0
Differencing scheme	Hybrid

Since the model equation may contain terms, which are not included in the PHOENICS general equation, they are implemented in PHOENICS by introducing the appropriate setting for each term in the Q1 file and applying extra FORTRAN coding in the GROUND subroutine.

In order to model the photocatalytic decolorization of textile dyes from the solution phase, a one-dimensional simulation was performed using PHOENICS package. The model input data are given in Table 2.

A one-dimensional finite volume model with a reactor length of 380 mm was divided into 50 equal size control volumes. The x-direction of Cartesian coordinate was used to simulate horizontal batch system in which photocatalytic decolorization process takes place. The number of time steps used was 12. Total iteration of 1000 was assigned to the simulation. The model was then run for a simulation time of 60 min. A molecular diffusion coefficient of 1×10^{-9} m^2/s was assigned for all dyes dissolved in solution system. All model input data were set through the Q1 file of PHOENICS package.

Figs. 1–3 compare experimental data and model predictions for the relative concentrations of RR, RBB and CB as a function of irradiation time respectively. The agreement between the predicted results and measured data are close. These figures were plotted for different H_2O_2 concentrations.

3.3. Mineralization of dyes

During the photocatalytic decolorization and mineralization of dye, various organic intermediates were produced. Consequently, destruction of the dye should be evaluated as an overall degradation process, involving the degradation of both the parent dye and its intermediates.

Further hydroxylation of aromatic intermediates leads to the cleavage of the aromatic ring resulting in the formation of oxygen-containing aliphatic compounds [10,16]. Carboxylic acids were

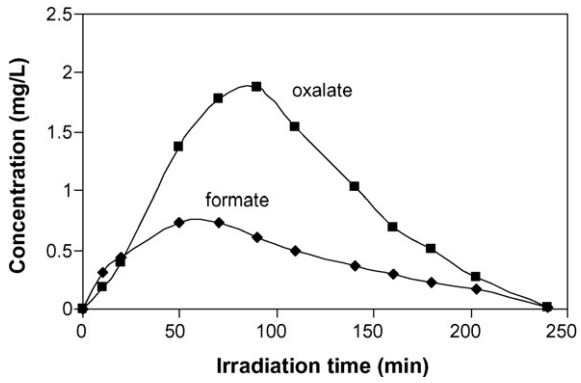

Fig. 4. Formation and disappearance of aliphatic carboxylic acids during the photocatalytic degradation of RR (Dye 50 mg/L, H_2O_2 450 mg/L).

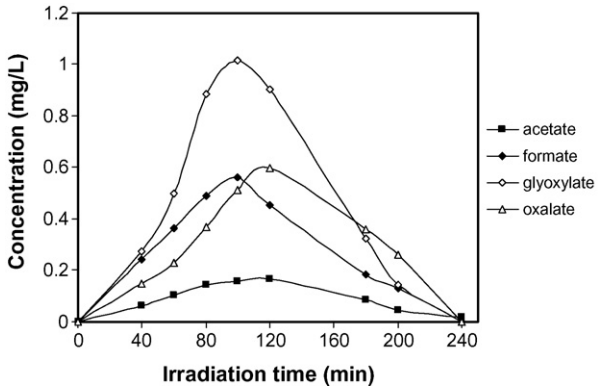

Fig. 5. Formation and disappearance of aliphatic carboxylic acids during the photocatalytic degradation of RBB (Dye 50 mg/L, H_2O_2 450 mg/L).

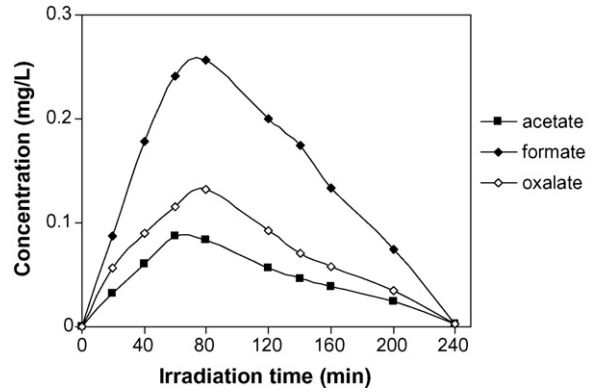

Fig. 6. Formation and disappearance of aliphatic carboxylic acids during the photocatalytic degradation of CB (Dye 50 mg/L, H_2O_2 300 mg/L).

detected as important aliphatic intermediates. Figs. 4–6 show the formation and disappearance of carboxylic acids with the irradiation time during the degradation of RR, RBB and CB, respectively. After 240 min of irradiation, carboxylic acids disappeared, indicating the mineralization of dye into CO_2 [35,36].

The chemical oxygen demand (COD) gives a measure of degradation of dye and generated intermediates during the irradiation [37] and also a measure of the oxygen equivalent of the organic content in a sample that is susceptible to oxidation by strong oxidant. After 3 h of irradiation, the COD removal efficiency of RR, RBB and CB were achieved 90, 91 and 90%, respectively.

4. Conclusion

This paper presents a computational fluid dynamics model using a multi-purpose commercial package called PHOENICS to simulate photocatalytic decolorization of textile dyes from aqueous solution by nanophotocatalysis using immobilized titania nanoparticle. The governing equation based on finite volume descretization scheme was used to numerically solve the mathematical equation describing decolorization process. Both experimental and modeling process showed that the dyes including CB, RR and RBB were successfully decolorized and degraded by this photocatalytic process. The rate of decolorization increased as the concentration of H_2O_2 increased from 50 to 1200 mg/L. A first-order model describes well the photocatalytic decolorization kinetics. The results of the model and the experimental method incorporating nanophotocatalysis using titania nanoparticle can help to design an appropriate environmental management strategy to minimize the adverse impacts caused by industrial wastes.

References

[1] N.M. Mahmoodi, M. Arami, N.Y. Limaee, N.S. Tabrizi, Decolorization and aromatic ring degradation kinetics of Direct Red 80 by UV oxidation in the presence of hydrogen peroxide utilizing TiO_2 as a photocatalyst, Chem. Eng. J. 112 (2005) 191–196.
[2] W. Yang, D. Wu, R. Fu, Effect of surface chemistry on the adsorption of basic dyes on carbon aerogels, Colloid Surf. A: Physicochem. Eng. Aspects 312 (2008) 118–124.
[3] N.M. Mahmoodi, M. Arami, N.Y. Limaee, Photocatalytic degradation of triazinic ring-containing azo dye (Reactive Red 198) by using immobilized TiO_2 photoreactor: bench scale study, J. Hazard. Mater. 133 (2006) 113–118.
[4] M. Arami, N.Y. Limaee, N.M. Mahmoodi, N.S. Tabrizi, Removal of dyes from colored textile wastewater by orange peel adsorbent: equilibrium and kinetics studies, J. Colloid Interf. Sci. 288 (2) (2005) 371–376.
[5] N.M. Mahmoodi, M. Arami, N.Y. Limaee, K. Gharanjig, F.D. Ardejani, Decolorization and mineralization of textile dyes at solution bulk by heterogeneous nanophotocatalysis using immobilized nanoparticles of titanium dioxide, Colloid Surf. A: Physicochem. Eng. Aspects 290 (2006) 125–131.
[6] M. Arami, N.Y. Limaee, N.M. Mahmoodi, N.S. Tabrizi, Equilibrium and kinetics studies for the adsorption of direct and acid dyes from aqueous solution by soy meal hull, J. Hazard. Mater. 135 (2006) 171–179.
[7] M. Arami, N.Y. Limaee, N.M. Mahmoodi, Investigation on the adsorption capability of egg shell membrane towards model textile dyes, Chemosphere 65 (2006) 1999–2008.
[8] X. Chen, S.S. Mao, Titanium dioxide nanomaterials: synthesis, properties, modifications and applications, Chem. Rev. 107 (7) (2007) 2891–2959.
[9] X. Chen, S.S. Mao, Synthesis of titanium dioxide (TiO_2) nanomaterials, J. Nanosci. Nanotechnol. 6 (4) (2006) 906–925.
[10] N.M. Mahmoodi, M. Arami, N.Y. Limaee, N.S. Tabrizi, Kinetics of heterogeneous photocatalytic degradation of reactive dyes in an immobilized TiO_2 photocatalytic reactor, J. Colloid Interf. Sci. 295 (2006) 159–164.
[11] A.C. Rodrigues, M. Boroski, N.S. Shimada, J.C. Garcia, J. Nozaki, N. Hioka, Treatment of paper pulp and paper mill wastewater by coagulation–flocculation followed by heterogeneous photocatalysis, J. Photochem. Photobiol. A: Chem. 194 (2008) 1–10.
[12] Y. Ao, J. Xu, D. Fu, X. Shen, C. Yuan, Low temperature preparation of anatase TiO_2-coated activated carbon, Colloid Surf. A: Physicochem. Eng. Aspects 312 (2008) 125–130.
[13] M. Bahgat, M.H. Khedr, S.A. Abdel-Moaty, Reduction kinetics, photocatalytic activity and magnetic properties of $CoFe_2O_4/BaFe_{12}O_{19}$ core/shell nanoparticles, Mater. Technol. 22 (2007) 139–146.
[14] B. Baeza, C. Lizama, C. Caneo, M. Ollino, Factorial design for the photodegradation of chloramphenicol with immobilized TiO_2, J. Adv. Oxid. Technol. 10 (2007) 411–414.
[15] A.F. Caliman, C. Cojocaru, A. Antoniadis, I. Poulios, Optimized photocatalytic degradation of Alcian Blue 8 GX in the presence of TiO_2 suspensions, J. Hazard. Mater. 144 (2007) 265–273.
[16] N.M. Mahmoodi, M. Arami, N.Y. Limaee, K. Gharanjig, F. Nourmohammadian, Nanophotocatalysis using immobilized titanium dioxide nanoparticle: degradation and mineralization of water containing organic pollutant: case study of Butachlor, Mater. Res. Bull. 42 (2007) 797–806.
[17] A.M.T. Silva, E. Nouli, N.P. Xekoukoulotakis, D. Mantzavinos, Effect of key operating parameters on phenols degradation during H_2O_2-assisted TiO_2 photocatalytic treatment of simulated and actual olive mill wastewaters, Appl. Catal. B: Environ. 73 (2007) 11–22.
[18] X. Lou, X. Jia, J. Xu, S. Liu, Q. Gao, Hydrothermal synthesis, characterization and photocatalytic properties of Zn_2SnO_4 nanocrystal, Mat. Sci. Eng. A: Struct. 432 (2006) 221–225.
[19] A. Aleboyeh, M.E. Olya, H. Aleboyeh, Electrical energy determination for an azo dye decolorization and mineralization by UV/H_2O_2 advanced oxidation process, Chem. Eng. J. 137 (2008) 518–524.
[20] M.M. Mohamed, I. Othman, R.M. Mohamed, Synthesis and characterization of MnO_x/TiO_2 nanoparticles for photocatalytic oxidation of indigo carmine dye, J. Photochem. Photobiol. A: Chem. 191 (2007) 153–161.
[21] N.M. Mahmoodi, N.Y. Limaee, M. Arami, S. Borhany, M. Mohammad-Taheri, Nanophotocatalysis using nanoparticles of titania: Mineralization and finite element modeling of Solophenyl dye decolorization, J. Photochem. Photobiol. A: Chem. 189 (2007) 1–6.
[22] M.A. Behnajady, N. Modirshahla, N. Daneshvar, M. Rabbani, Photocatalytic degradation of an azo dye in a tubular continuous-flow photoreactor with immobilized TiO_2 on glass plates, Chem. Eng. J. 127 (2007) 167–176.
[23] L.-C. Chen, C.-M. Huang, F.-R. Tsai, Characterization and photocatalytic activity of K^+-doped TiO_2 photocatalysts, J. Mol. Catal. A: Chem. 265 (2007) 133–140.
[24] J. Saien, A.R. Soleymani, Degradation and mineralization of Direct Blue 71 in a circulating upflow reactor by UV/TiO_2 process and employing a new method in kinetic study, J. Hazard. Mater. 144 (2007) 506–512.
[25] N.M. Mahmoodi, M. Arami, Bulk phase degradation of Acid Red 14 by nanophotocatalysis using immobilized titanium (IV) oxide nanoparticles, J. Photochem. Photobiol. A: Chem. 182 (2006) 60–66.

[26] J. Marugán, M.-J. López-Muñoz, W. Gernjak, S. Malato, Fe/TiO_2/pH interactions in solar degradation of imidacloprid with TiO_2/SiO_2 photocatalysts at pilot-plant scale, Ind. Eng. Chem. Res. 45 (2006) 8900–8908.
[27] V. Luca, M. Osborne, D. Sizgek, C. Griffith, P.Z. Araujo, Photodegradation of methylene blue using crystalline titanosilicate quantum-confined semiconductor, Chem. Mater. 18 (2006) 6132–6138.
[28] T. Takeda, I. Oyane, K. Okitsu, M. Furuta, H. Bandow, R. Nishimura, Y. Maeda, Toxicity evaluation of sonochemical decomposition products of chloroacetone to yeast cells by calorimetric analysis, Bunseki Kagaku 55 (2006) 701–706.
[29] N.M. Mahmoodi, M. Arami, N.Y. Limaee, K. Gharanjig, Photocatalytic degradation of agricultural *N*-heterocyclic organic pollutants using immobilized nanoparticles of titania, J. Hazard. Mater. 145 (2007) 65–71.
[30] M.R. Hoffmann, S.T. Martin, W. Choi, D.W. Bahnemann, Environmental applications of semiconductor photocatalysis, Chem. Rev. 95 (1995) 69–96.
[31] I.K. Konstantinou, T.A. Albanis, TiO_2-assisted photocatalytic degradeation of azo dyes in aqueous solution: kinetic and mechanistic investigations. A review, Appl. Catal. B: Environ. 49 (2004) 1–14.
[32] A.K. Ray, A.A.C.M. Beenackers, Novel photocatalytic reactor for water treatment, AIChE J. 44 (2) (1998) 477–483.
[33] CHAM, The PHOENICS On-Line Information System, www.cham.co.uk/phoenics/d_polis/polis.htm, 2000.
[34] APHA, Standard Methods for the Examination of Water and Wastewater, 17th ed., American Public Health Association, Washington, DC, 1989.
[35] N.M. Mahmoodi, M. Arami, K. Gharanjig, F. Nourmohammadian, A.Y. Bidokhti, Purification of water containing agricultural organophosphorus pollutant using titania nanophotocatalysis: laboratory studies and numerical modeling, Desalination 230 (2008) 183–192.
[36] A. Houas, H. Lachheb, M. Ksibi, E. Elaloui, C. Guillard, J.M. Hermann, Photocatalytic degradation pathway of methylene blue in water, Appl. Catal. B: Environ. 31 (2001) 145–157.
[37] J. Li, C. Chen, J. Zhao, H. Zhu, J. Orthman, Photodegradation of dye pollutants on TiO_2 nanoparticles dispersed in silicate UV–vis irradidtion, Appl. Catal. B: Environ. 37 (2002) 331–338.